System for measuring the spatial reflectance distribution of material surfaces

L A Berni, M S Ribeiro, T F Paes and A F Beloto
Instituto Nacional de Pesquisas Espaciais (INPE), Laboratório Associado de Sensores e Materiais (LAS). Av. dos Astronautas, 1758, São José dos Campos/SP, Brazil 12227-010

E-mail: berni@las.inpe.br

Abstract. An automatic device for measuring the reflectance distribution from material surfaces was assembled in the laboratory. The mechanical setup employs two aluminum rotating arms driven by stepper motors: one for the light source and the second for the collecting optics. The two arms can rotate in the zenith direction from -90 to +90 degrees and the light collecting arm in the azimuth angle over 360 degrees, both with adjustable angular resolution. Measurements from black anodized aluminum, PTFE, graphite, porous silicon and a lambertian reference surface were performed to validate the system.

1. Introduction

The interaction of light with an object surface can be represented as a single function, called Bidirectional Reflection Distribution Function (BRDF)[1, 2]. That describes the pattern of light reflected from a material surface to all directions of incident light. The BRDF is defined as the ratio of reflected radiance (W m^{-2} sr^{-1}) to the incident irradiance (W m^{-2}) on the surface, see Eq. (1). It is a five dimensional function f(θ_i, φ_i, θ_r, φ_r, λ), where θ_i is the incident zenith angle, θ_r is the reflected zenith angle, φ_i and φ_r are the incident and reflected azimuth angles respectively, and λ the measured wavelength. For simplicity, the polarization dependence of light was left out of the equation as our system employs an unpolarized light source. A standard reflectance from GetSpec (GetReflex) was used to determine the irradiance on the samples surface for each incident angle of the light beam.

$$f(\theta_i, \varphi_i, \theta_r, \varphi_r, \lambda) = \frac{dL_r(\theta_r,\varphi_r,\lambda)}{dE_i(\theta_i,\varphi_i,\lambda)} \quad (1)$$

The characterization of the reflective properties of a surface by BRDF measurements and theoretical models are widely used in computer graphics to generate realistic images of virtual objects. The knowledge of these reflective properties can also be used in optical system designs in the analysis and reduction of stray light improving the signal to noise ratio. There are several analytical models that mathematically describe this interaction more or less complete, such as, Lambert model (ideal diffuse), Phong (Blinn-Phong) [3], Oren-Nayar [4] And Cook-Torrance [5].

The reflectance profiles measured in the laboratory can be used both to validate the models described above and also as input data in optical simulation programs. In an optical design which seeks to optimize the signal to noise ratio is essential to know how each material surface that makes up the system scatters radiation. Thus, it is possible to determine the critical regions and choose the best material and finishing for every situation. Normally, we use materials that have a high rate of absorption in the wavelength

region of spurious radiation, but if the materials must display characteristics like specular, diffuse or intermediate depends on each situation. The development of the system described here was motivated by the study of stray light in optical systems [6], the input optics of radiometers [7] and porous silicon as coatings for solar cells [8].

2. System set up and specifications

The system was completely assembled on a structure of area of 1100mm x 800mm and height of 900mm. The mechanical setup employs two aluminum rotating arms, one for the 50W halogen light source and the second for the lens-fiber collecting optics. In the illumination arm there are two 40 mm diameter apertures to partially collimate the light beam. The rotation radius of this arm is 320 mm. The collecting light arm was assembled with one lens of 50 mm diameter and focusing length of 40 mm that projects the collecting area from the sample surface on a fiber bundle of 3.0 mm diameter. The rotation radius of this arm is 210 mm. The two arms can rotate in the zenith direction from -90 to +90 degrees and the light collecting arm in the azimuth angle over 360 degrees. All three axes are driven by three 18 kgf.cm stepper motors with adjustable angular resolution. The wavelength of the scattered collected light can be selected by a set of interference filters from 300nm to 1100nm with an average bandwidth of 8.0 nm. The signal is detected by a Si photodiode detector (Oriel 70336) connected to a lock-in amplifier (Oriel-Merlin) and after, the signal is transferred to the computer by a A/D converter (NI USB-6210). The sample to be measured is positioned on an adjustable table so that its surface is on the center of rotation of the optical system. Figure 1 shows the design of the assembled system.

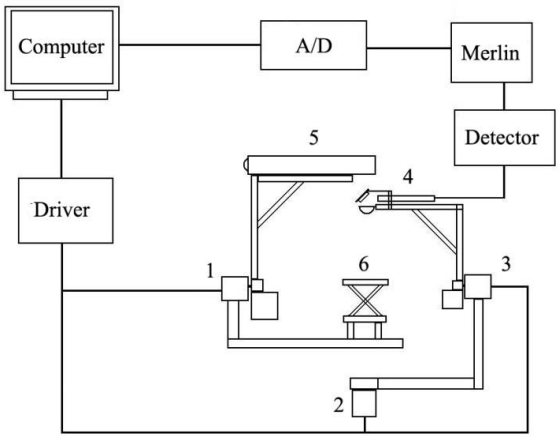

Figure 1. Schematic drawing of the system: 1, 2 and 3 - stepper motors; 4 – collecting scattered light arm; 5 – source light arm and 6 – sample adjustable table.

To characterize the system, it was measured the spectrum of the light source, the spatial irradiance distribution on the sample surface, the spot size of illumination and observation as a function of the incident light angle. Figure 2 (left) shows the irradiance on the center position on the surface table for an incident angle of 0^o (the illumination is right above the sample surface). The wavelength dependence was measured with a compact CCD spectrometer from Getspec model 2048 from 250 nm to 1100 nm. As seen in figure 2 (left), the profile is a typical spectrum of a halogen dichroic lamp with the maximum irradiance at 640 nm. For the same incident angle, it was measured the spatial irradiance distribution over the sample table as shown in figure 2 (right). The maximum variation of the irradiance over the center region of 40 mm diameter is 4%. As the angle of the incident light increases from 0^o to $\pm 90^o$ the size of the illumination spot increases as shown in figure 3(left). The spot of collection optics was measured illuminating the fiber optic from the detector side with a HeNe laser. The projected area over

the sample table was measured from -80º to 80º as shown in Fig. 3 (right). For the arm at 0º the collection area of the optics is about 10mm and increase up to 13.5mm at ± 40º. Since the observation spot size must be lesser than the sample diameter, this graph shows the limits of the zenith angle to be measured.

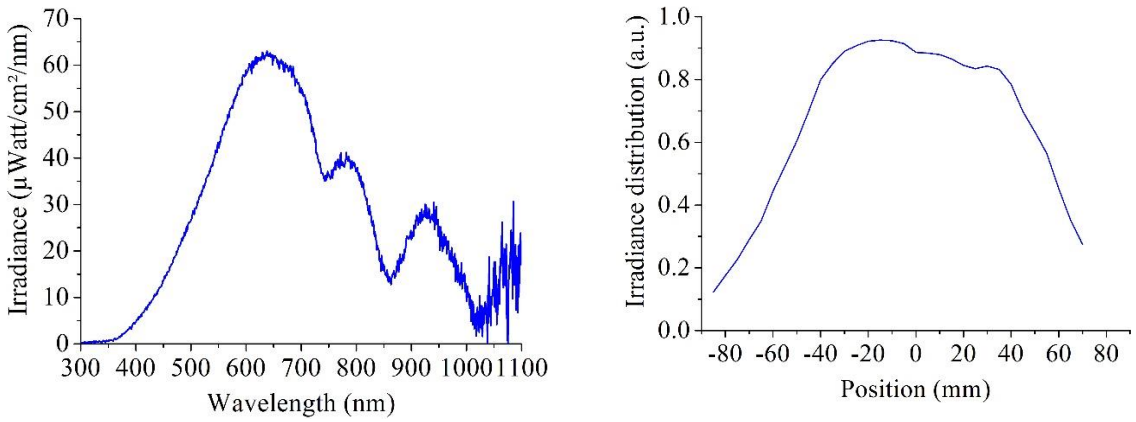

Figure 2. Left: Spectrum irradiance of the light source. Right: Spatial distribution of the irradiance on the sample position.

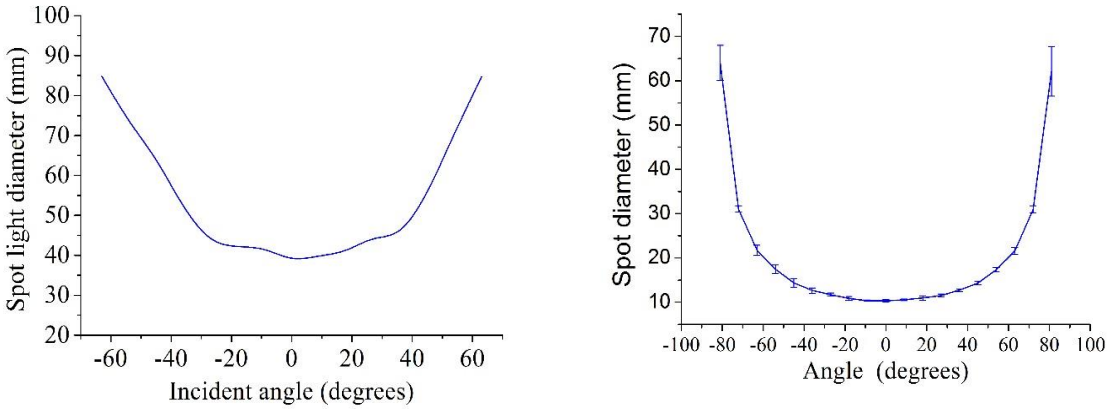

Figure 3. Spot diameter as a function of angle. Left: Incident light. Right: Scattering light.

3. Results

In order to verify the system, some surfaces usually employed in the laboratory were measured as shown in the following figures. In all the figures, the light beam is incident at the right side of the graph box with an angle of incidence measured from the vertical through the point (0,0). All these measurements were performed at the wavelength of 550nm. The scattered light was collected in the zenith plane from -80º to 80º and in the azimuth over 340º in steps of 10º. The face of the samples were positioned in the XY plane at position (0,0) and the relative scattered signal is indicated in the vertical Z axis. Figure 4 (left) shows the BRDF measured from our standard reflectance at 15º of incidence. Since this surface has a lambertian profile, this measurement was used to determine the incident irradiance for each angular position. In the figure there are some lost points due to the shadow of the detector arm at the positions where it passes in front of the light arm. Figure 4(right) shows the scattering distribution for a PTFE sample at the same incidence with step in the azimuth of 30º. PTFE is also used

as a reference of reflectance surface, but in this case this sample presents a polished finishing surface that explain the increased signal at the specular reflection position. In the laboratory the PTFE is used as a diffuser for the entrance optics of radiometers.

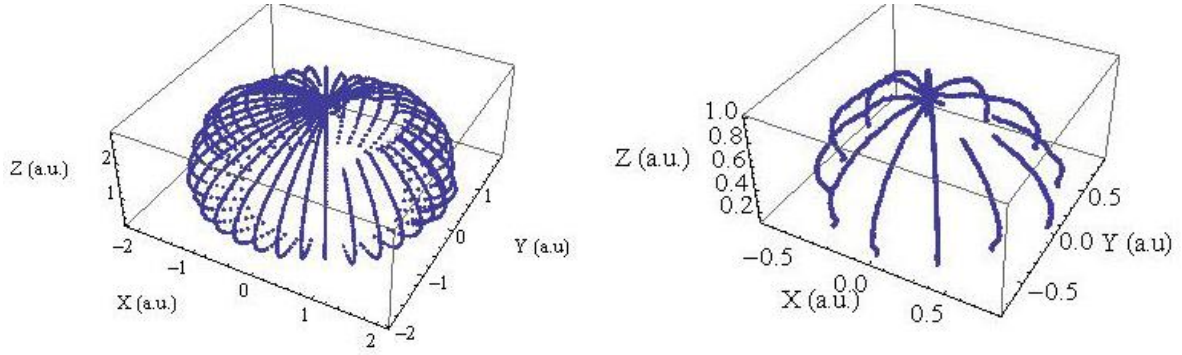

Figure 4. BRDF for standard reference (left) and PTFE (right) at 15º of incidence.

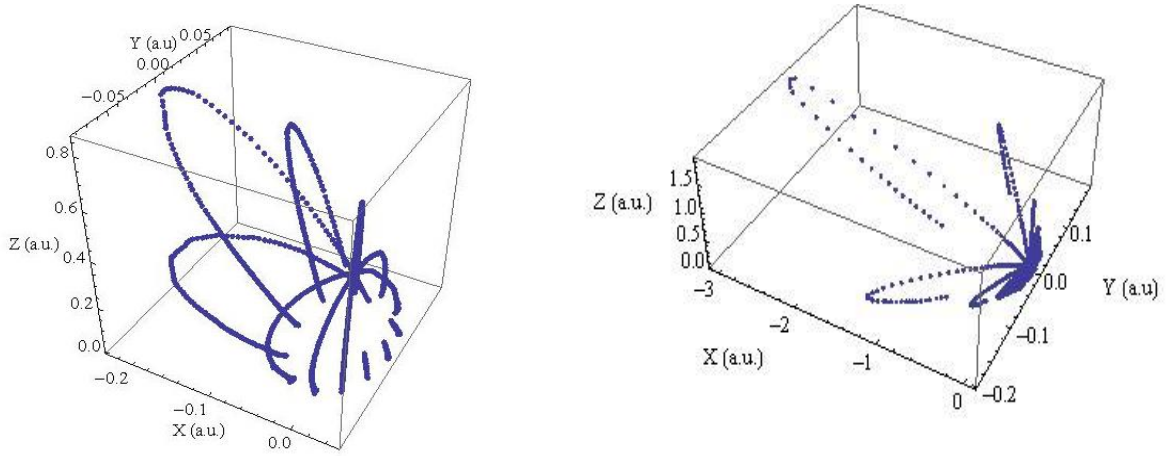

Figure 5. Left: BRDF for graphite sample at 15º of incidence and azimuth step of 30º. Right: graphite sample at 60º of incidence and azimuth step of 10º.

Figure 5 shows the scattering profile of a graphite sample that in some situations is used to control the stray light of optical systems [6]. For incidence at low angle, the sample shows a diffuse scattering profile which can complicate the control of stray light. For the same sample at 60º, the profile shows a lower diffuse signal and a high signal at the specular position. Figure 6 shows the profiles for black anodized aluminum at the same previous angles, which shows that it is possible to have a better control of the stray light at low angles with this sample. Figure 7 shows the BRDF for porous silicon samples at the same incidence angles. For these measurements, the zenith angle was limited from -60º to 60º due the small size of the samples and the azimuth step of 10º. These first measurements of this kind of sample, show profiles that could be explained by the complex structure of the surface of the porous silicon that will be the focus of the next study. Figure 8 shows BRDF measurements for graphite and black anodized aluminum samples at several angles of incident light for wavelengths of 550 nm and 900 nm. These measurements were performed at the same plane of incident light beam. The results show that the two samples present higher reflectance for near infrared wavelength and the reflectance signal increases with the incident angle. Comparing these results with the previous ones, it is possible to conclude that the black anodized aluminum sample is better for stray light mitigation with reflectance

three times lesser than the graphite sample.

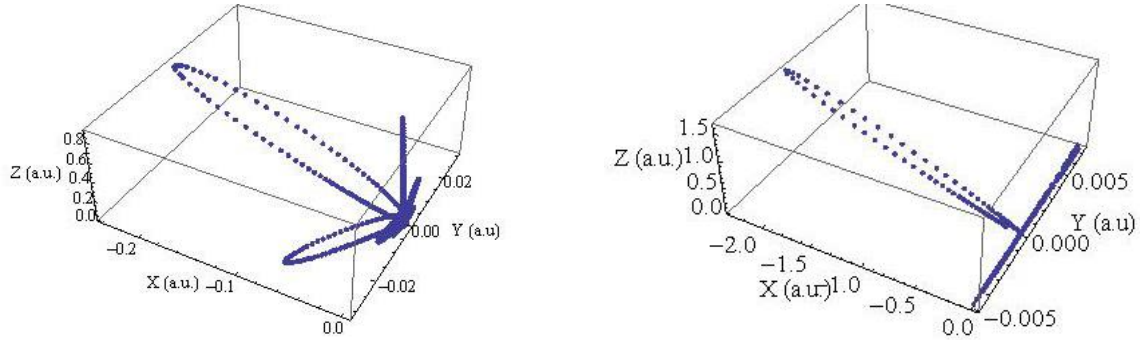

Figure 6. BRDF for black anodize aluminum sample at 15º of incidence (left) and 60º (right).

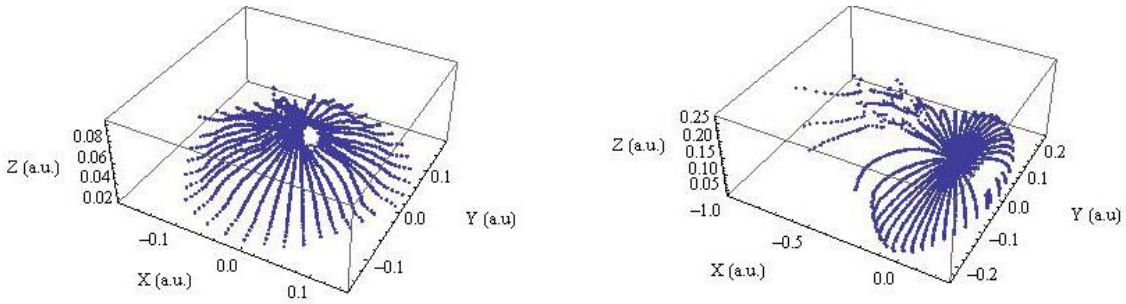

Figure 7. BRDF for porous silicon sample at 15º of incidence (left) and 60º (right).

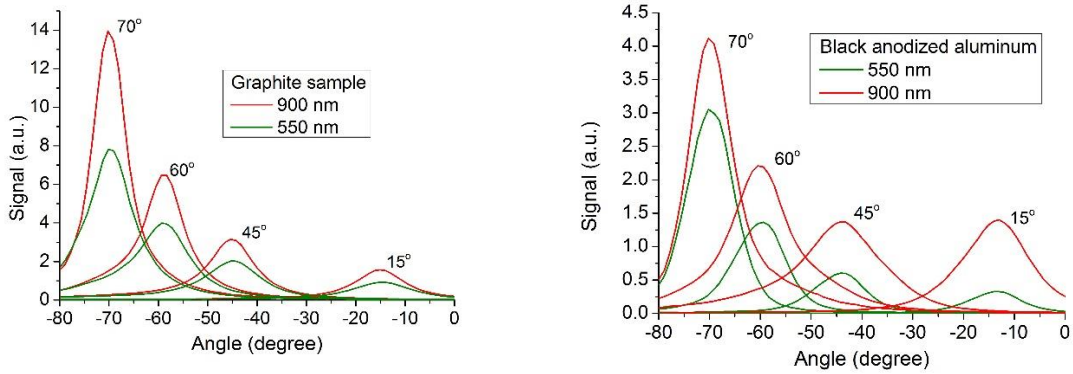

Figure 8. BRDF for several incident angles at 900nm and 550nm for graphite (left) and black anodized aluminum (right).

4. Discussion and conclusions

A system for measuring the BRDF from samples surface was implemented in the laboratory. The profiles of measured surfaces showed a clear dependence on surface finishing and with angle of incidence of radiation, which will be the focus of the next study as well as the dependence with the wavelength. Regarding to the porous silicon, we will attempt to verify the correlation between the profiles of the BRDF and the different porous structures of the material. To improve the irradiance on the sample surface, the light source will be changed by a QTH lamp powered by a radiometric power

supply with a liquid light guide to drive the beam to the illumination arm. The spectral detection of scattered radiation will be changed by a compact CCD spectrometer to measure the wavelength radiation between 250 and 1100 nm at the same time.

Acknowledgments
The authors Mario S. Ribeiro and Tiago F. Paes are grateful to CNPq and CAPES, respectively, for the fellowships. The authors thank CAPES for the financial support to attend the ICO 23 congress.

References

[1] Nicodemus F E. Directional reflectance and emissivity of an opaque surface 1965 *Applied Optics* **4** No. 7.
[2] Martonchik J V, Bruegge C J and Strahler A H. A Review of reflectance nomenclature used in remote sensing 2000 *Remote Sensing Reviews* **19** pp. 9 – 20.
[3] Blinn J F. Models of light reflection for computer synthesized pictures 1977 *Proceedings of the 4th Annual Conference on Computer Graphics an Interactive Techniques* pp192-198.
[4] Oren M and Nayar S K. Generalization of Lambert`s reflectance model 1995 *International Journal on Computer Vision* **14** 3 pp227-251.
[5] Cook R L and Torrance K E. A reflectance model for computer graphics 1981 *Computer Graphics* **15** 3 pp307-316.
[6] Berni L A , Albuquerque B F C. Stray light analysis for the thomson scattering diagnostic of the ETE tokamak 2010 *Review of Scientific Instruments* 81, 123504.
[7] Berni L A, Vilela W A and Beloto A F. Otimização da ótica de entrada por traçado de raios no desenvolvimento de um radiômetro UV 2011 *Revista Brasileira de Energia Solar* **2**, série 1 ISSN 2178-9606.
[8] Ramizy A, Aziz W J, Hassan Z, Omar K and Ibrahim K. Improved performance of solar cell based on porous silicon surfaces 2011 *Optik* 122 2075 - 2077.